THE EFFECT OF INTEGRAL STIFFENING ON THE FATIGUE OF THIN-WALLED PLATES SUBJECTED TO SHEAR

Łukasz Święch

Faculty of Mechanical Engineering and Aeronautics, Rzeszów University of Technology,
al. Powst. Warszawy 8, 35-959 Rzeszow, Poland

Abstract

The paper presents results of experimental investigations of fatigue behaviour of thin-walled integrally stiffened plates. Structures under consideration was treated as the skin part of the semi-monocoque construction and subjected to shear load what led to the post-buckling state of deformation. Tested plate was manufactured as an integral construction from 2024-T3 aluminium alloy with use of the CNC milling machine. Experimental results of preliminary static test in the form of displacement fields obtained by the digital image correlation method were compared to the results of numerical calculations. On the basis of this comparison, the correctness of the stress distribution obtained by numerical method was found and the load level for fatigue test was chosen. The conducted experimental tests showed a significant influence of the stiffener arrangement on the form of fatigue failure.

Keywords: *thin-walled structures, integrally stiffened structures, post-buckling, nonlinear deformations, fatigue tests, digital image correlation, finite element analysis*

1. INTRODUCTION

In order to obtain an advantageous weight-to-strength ratio of the load-bearing elements, so-called semi- monocoque structures are commonly used in many technical fields. A special feature of this type of load-bearing structures is their division into a relatively thin skin, whose task is to transfer shear stress and a number of longitudinal and transverse elements forming the structure's skeleton and responsible for transferring other forms of load and maintaining the geometry [1,2]. Such thin-walled structures, are exposed to the loss of stability, which causes a change in the nature of their operation due to large, non-linear deformations of a geometric nature [3]. It should be noted that in the case of aviation structures, the local loss of stability of the skin in terms of operational loads is permissible.

Continuous development of production methods and construction materials enable the construction of more and more geometrically complex structures that increase the strength-to-weight ratio. This tendency is manifested, inter alia, in the use of integral structures, in which a relatively thin skin is reinforced with a series of ribs constituting an integral part of the structural element. Such issues have become the subject of research in the field of application of longitudinal stiffeners [4-6] and isogrid stiffeners [7, 8]. In addition to determining the static strength, in the case of aviation structures, fatigue tests are particularly important, which remain permanently valid due to the safe operation of aircraft and their most important elements [9, 10].

The work considers the behaviour of structures subjected to fatigue loads in the field of post-critical deformation. A solution of this type may be an alternative to the currently used thin sheet metal coverings. The use of integral stiffeners makes it possible to reduce the weight of the structure while maintaining its critical load level. The second approach is to increase this load value while maintaining the weight of the structure. In each of these cases, however, it is extremely important to determine the effect of stiffeners on the service life, which determines the actual usefulness of the considered design solution.

The presented research was divided into two stages. In the first stage, experimental static tests were carried out, which made it possible to determine the influence of stiffeners on the value of the critical load. The test results were compared with the results of numerical calculations in terms of FEM. In the next step, the plate under consideration was subjected to fatigue tests in order to demonstrate the effect of integral stiffeners on the fatigue strength.

2. THE OBJECT OF THE STUDY

The integrally stiffened rectangular plate was chosen for experimental investigation and numerical analysis. Geometry of the plate with overall dimensions of 340 mm by 260 mm is presented in figure 1. The plate was manufactured with aluminium alloy 2024 T3 as integral structure stiffened by 15 prismatic ribs 1 mm thick and 5 mm high. The thickness of the plate was 0.75 mm what leads to mass of 219 grams. As a reference structure with equivalent mass (232 g), a smooth plate with a thickness of 1 mm and identical overall dimensions was chosen. All subsequent considerations and their results were conducted in relation to the reference structure.

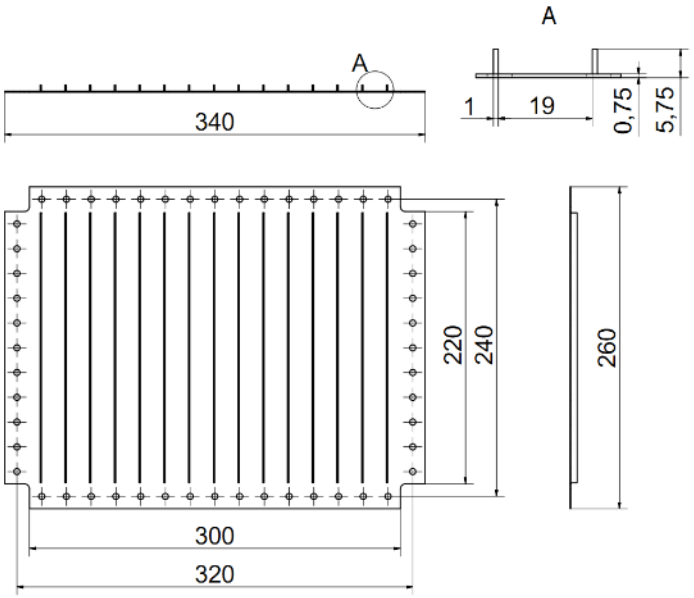


Fig. 1. Geometry of the plate

The plate was machined with the use of CNC milling machine and specially prepared vacuum table (Fig. 2). The use of a table was necessary to ensure high geometrical tolerance of the manufacturing process. Figure 3 presents nominal relations between stress and strain for duralumin 2024 T3 used in the manufacturing of tested samples. Table 1 presents material properties and constants for chosen alloy.

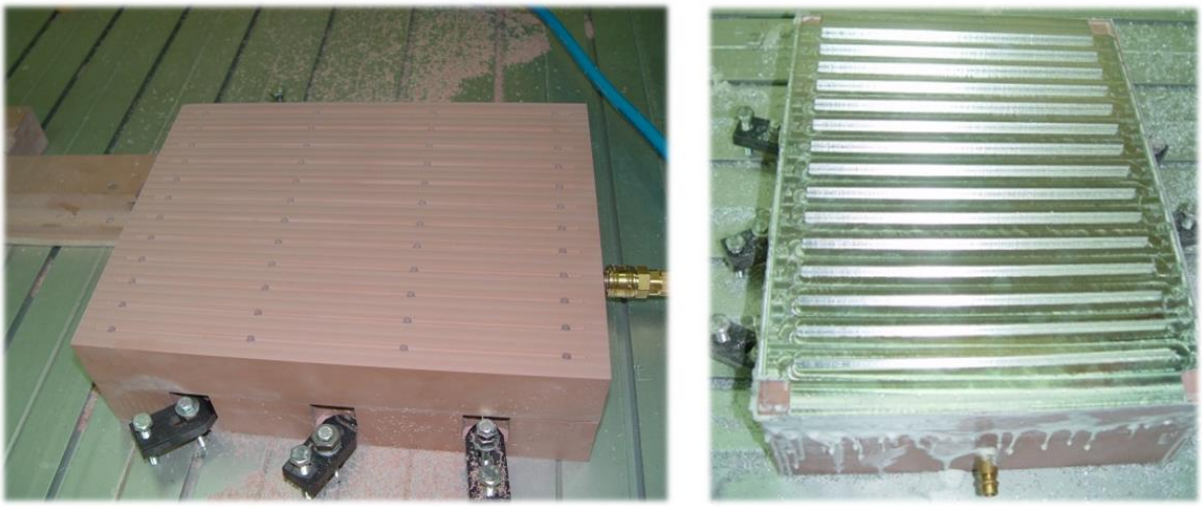


Fig. 2. Vacuum table used in the manufacturing process and finished test plate

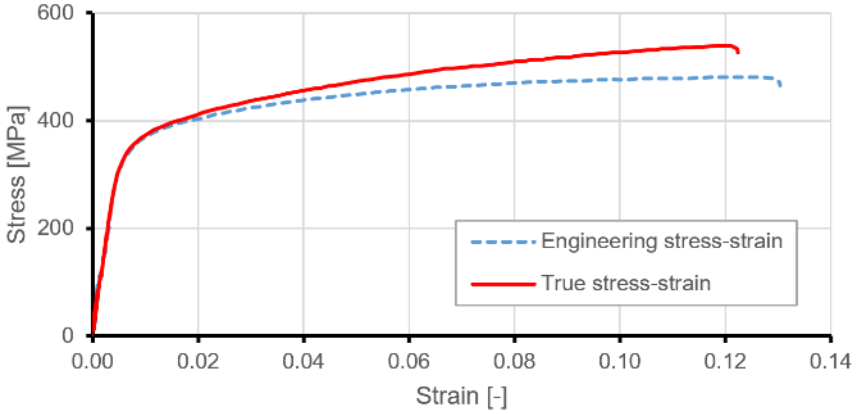


Fig. 3. Nominal stress–strain curves for 2024 aluminium alloy

Parameter name	Young Modulus E, GPa	Poisson Ratio, -	Ultimate Tensile Stress R_m, MPa	Yield Stress $R_{p0.2}$, MPa
Value	70	0.33	488	345

Table 1. The basic mechanical properties of 2024-T3 aluminium alloy

3. EXPERIMENTAL TEST STAND

During the experimental research, the plate was subjected to the pure shear loading condition. The plate was mounted in the steel, hinged frame which transferred vertical force from the strength machine into the pure shear on the edges of the plate (Figure 4). Experimental static and low cycle fatigue tests were conducted with the use of universal strength testing machine Zwick-Roell Z050. The force level control was used with assumption that this kind of loading is closest to the real operational condition of the structure. During the research, the plate was subjected to load up to 25 kN, which resulted in post-critical deformations. Figure 5 presents manufactured plate mounted in the test area of the machine.

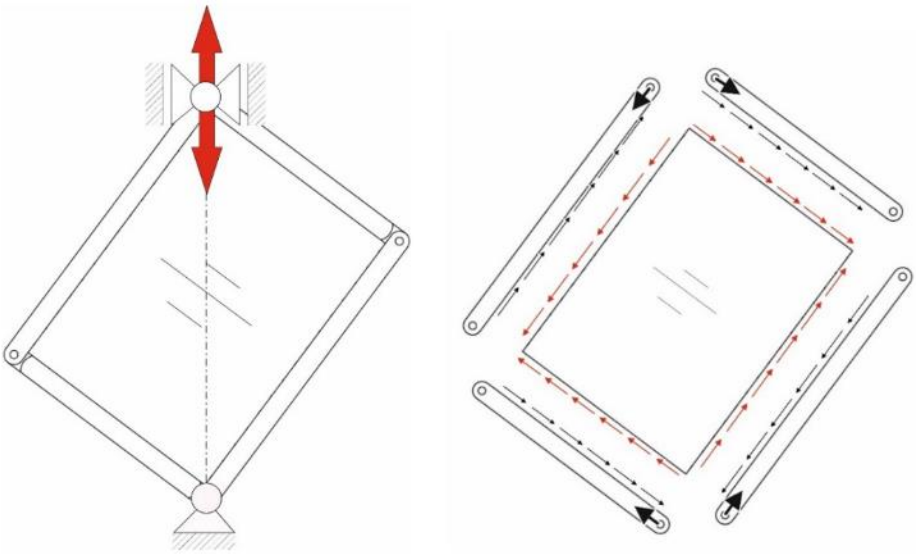


Fig. 4. Loading conditions acting on the plate

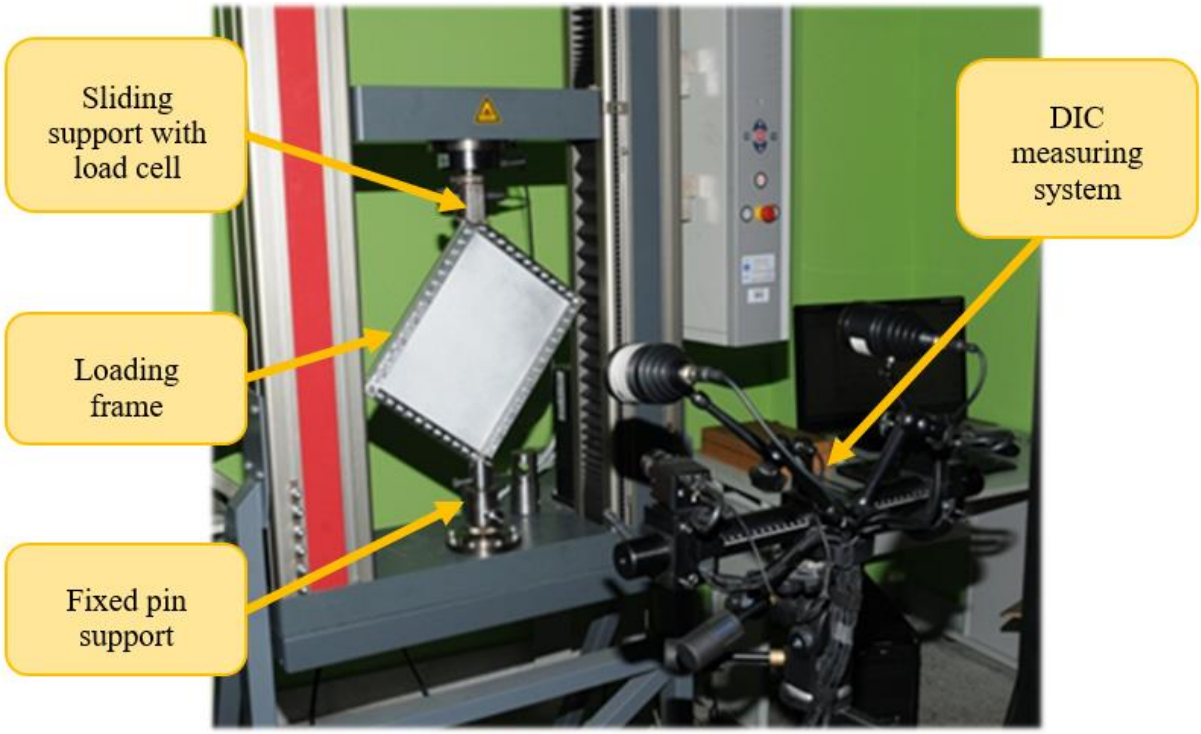


Fig. 5. Plate mounted in the test area of the strength machine and ARAMIS scanner (plate shown from unstiffened side)

A three-dimensional Digital Image Correlation (DIC) system GOM ARAMIS was used during the experiment. ARAMIS is a non-contact and material-independent measuring system which allows to capture and analyse deformations of the measured object in consequent load steps over time [11, 12]. Measurements with the use of the ARAMIS system consist of taking a series of images of the specially prepared object. Preparation involves covering of measurement surface with a stochastic pattern of black spots (Fig. 6). Two stereo-metrically arranged digital cameras are used to record the displacements of spots related to strain changes due to the increase in loading. The quality of the pattern has also a significant influence on the accuracy of results.

During the test, displacements fields were recorded on the unstiffened side of the plate with the frequency of 1Hz. The analogue electrical connection between testing devices allowed to assign the information of acting load in every step of deformation.

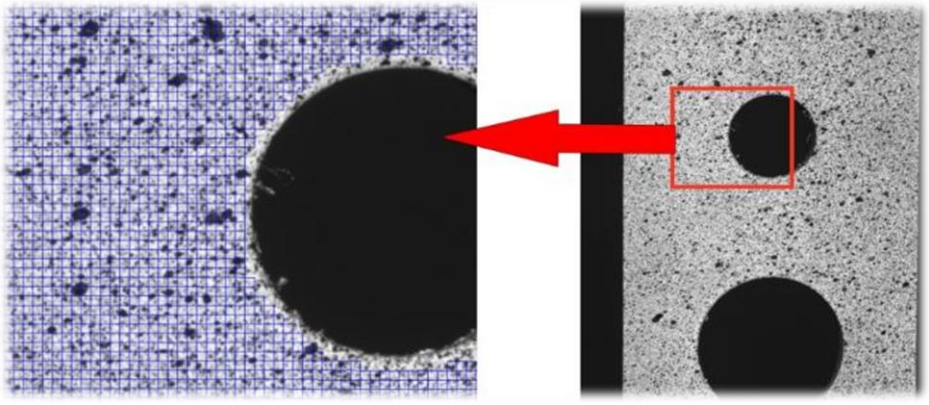


Fig. 6. Sample of the surface prepared for DIC measurement and division into the sub-areas used in the strain calculations

4. NUMERICAL ANALYSIS

Numerical analyses was conducted with use of the commercial finite element software Abaqus [13]. Numerical model of the plate was developed with use of the four nodes S4R shell elements with reduced integration and large-strain formulations standard library shell elements. Steel frame members were modelled with beam B31 elements. Frame members were connected together with use of the MPC – Hinge type elements and frame to the plate connection was realized by the TIE type of connection. Boundary conditions was placed on the bottom and upper node of the frame. For a comparison of results, a second model consisting of a smooth plate with equivalent mass was developed.

Nonlinear numerical analyses were carried out with the use of modified prognostic Newton–Raphson procedures with standard load corrections [14-16]. The first step of analysis for both stiffened and smooth plates involved a simplified, linearized analysis of stability. Results of the linear buckling analyses were aimed at predicting the critical load and shape of the deformation field, which was used next as the initial imperfection of the structure.

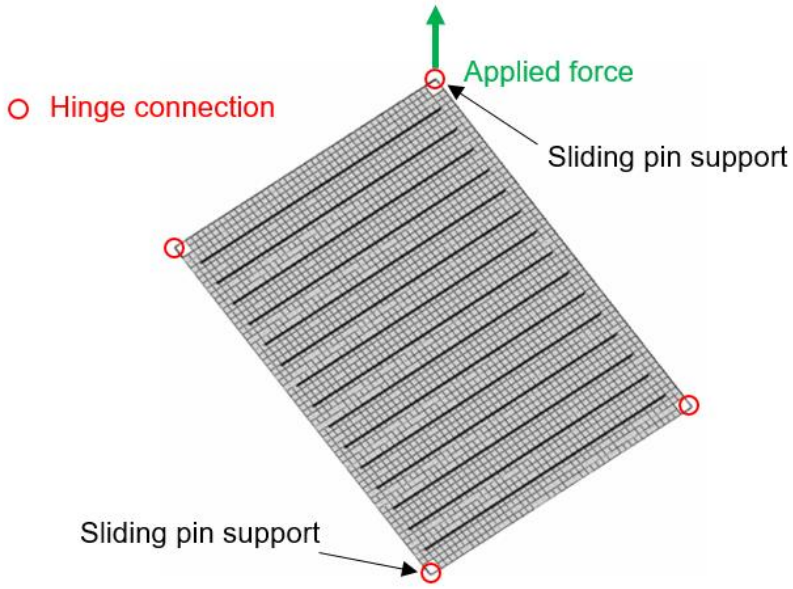


Fig. 7. FEM model and boundary conditions

5. RESULTS OF STATIC TEST AND COMPARISON TO FEM CALCULATIONS

As mentioned above, the reference structure was the smooth plate with the thickness of 1 mm and equivalent mass to the stiffened plate under consideration. Numerical analyses showed an increase of 203% in the critical load level for the stiffened plate. Exact values of critical loads for smooth plate and integral one were 5.7 kN and 17.3 kN respectively.

Figure 8 presents a comparison of the deflection area of integral plates obtained through experimental tests and numerical FEM analyses. The discrepancy in the results is caused by the fact that under a high load of the system (25 kN), the identified axial clearance between the frame elements and the upper node of the testing machine caused a slight rotation of the plate around the axis of force application, hence, in Figure 8 in the upper left corner of the plate, the deflection is visible equal to 0.55 mm, which is not reasonably reflected in the numerical model. Taking the above into account, the maximum plate deflection turned out to be close to the result of numerical analyses.

On the basis of the obtained results, the distribution of stress effort based on H-M-H hypothesis, obtained by numerical analyses was considered reliable. A decrease in the stress effort value for stiffened plate was observed amounting to 43% (Fig. 9b). The stress in the case of a ribbed plate constitute only 62% of the value assumed as the yield stress (Re = 345 MPa), while for a smooth plate, these stresses exceed the value of Re by 30 MPa, which is approx. 9% of the value of stress causing permanent deformation.

The comparison of the H-M-H stress distribution is also interesting. There is a clear change in its character. The stress gradient drops almost twice as compared to a smooth plate. Under these conditions, the active working area of the plate increases.

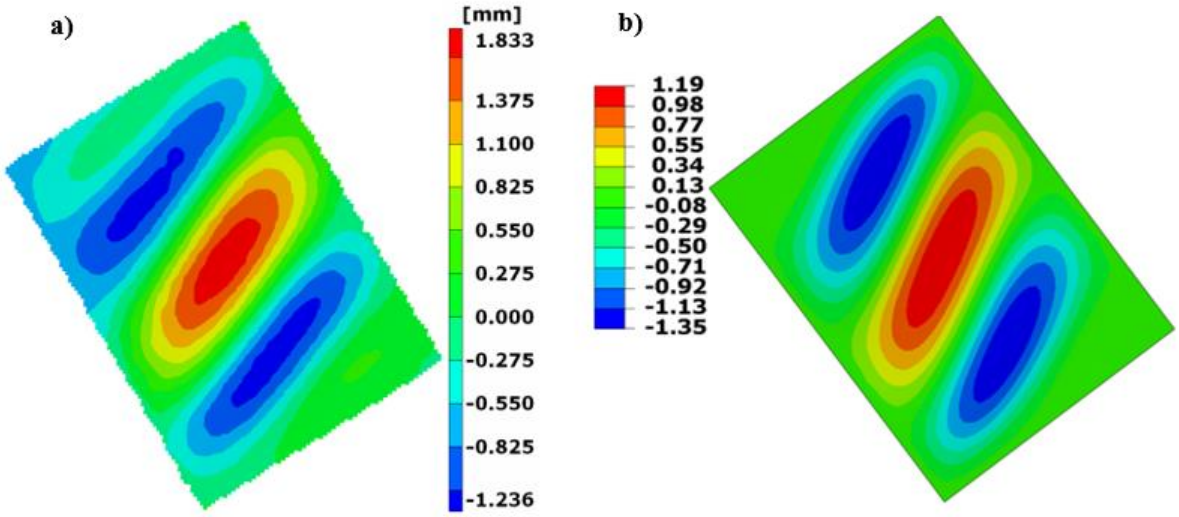


Fig. 8. Deflection of the plate surface under load equal to 25 kN
a) experimental result captured by DIC scanner, b) result of FEM calculations

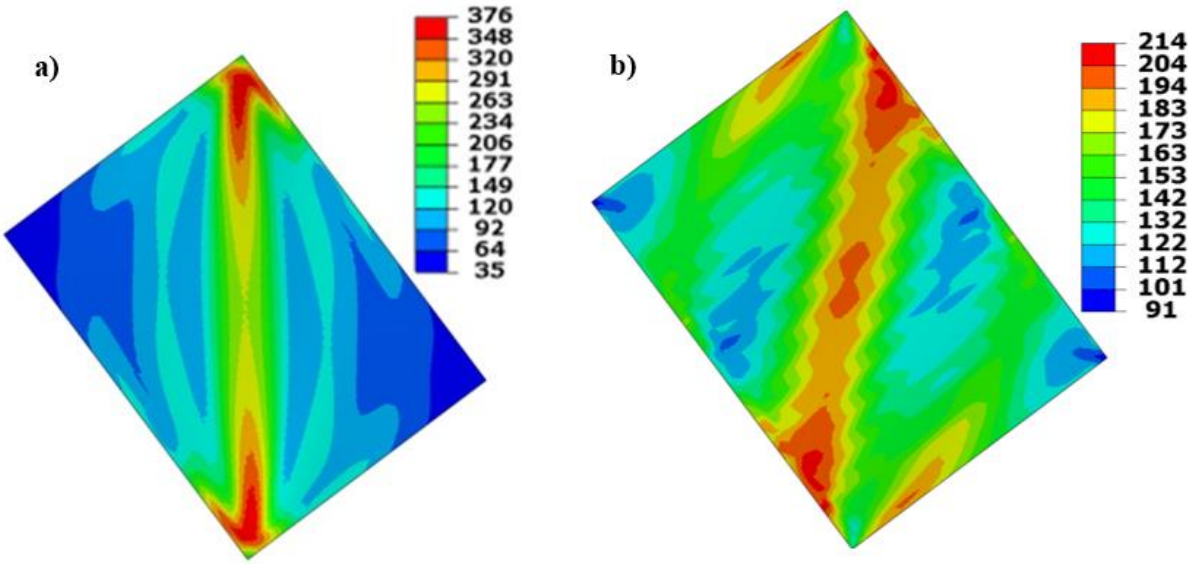


Fig. 9. H-M-H stress distribution [MPa] under load level of 25 kN

a) smooth plate, b) integrally stiffened plate

6. FATIGUE TEST

In order to determine the durability of the ribbed structure and the effect of stiffeners on the nature of the progressive failure, fatigue tests were carried out. The load spectrum (Fig. 10) was assumed as monocyclic *saw-tooth* cycles with the upper limit of the force equal to 25 kN. The load caused the stress

level in the structure to be about the 60% of the yield point of the material from which the panel was made.

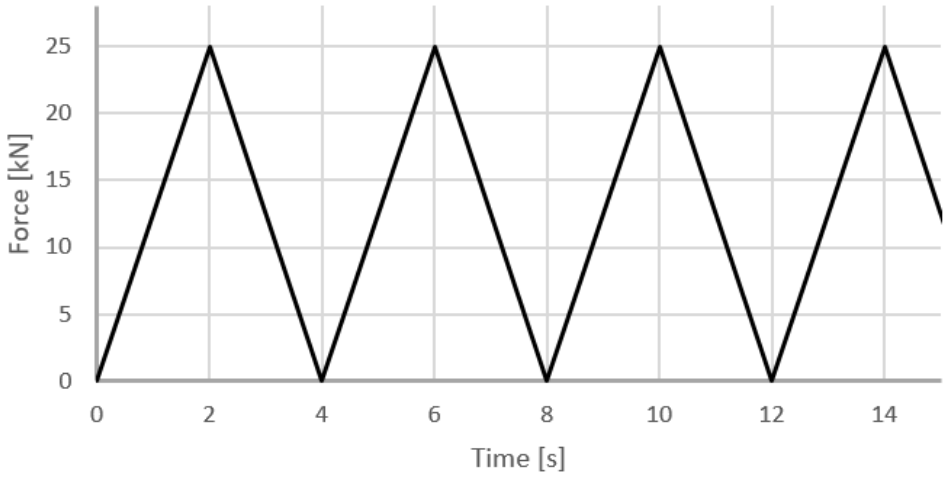


Fig. 10. Fatigue load spectrum

The first cracks in the zone of the highest stress were observed after approx. 10000 cycles (Fig. 11, 12). Further cracks observed during the next almost 7000 load cycles led to the destruction of the structure after 16 740 cycles. The form of destruction presented in figure 13 showed that the stiffening ribs played the role of the so-called crack arrester, influencing the direction of fatigue crack development and keeping it in one zone, between two stiffeners.

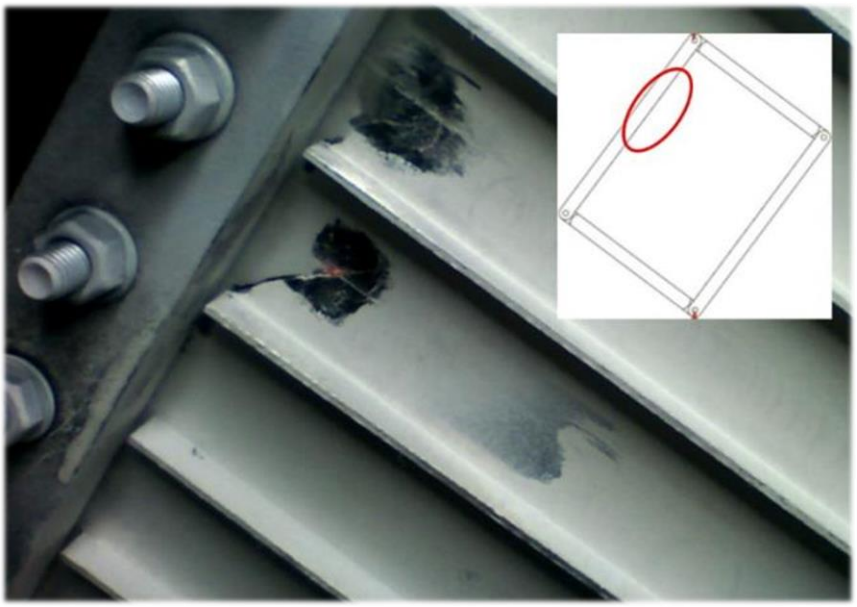


Fig. 11. Fatigue cracks and their location on the plate surface. View from stiffened side

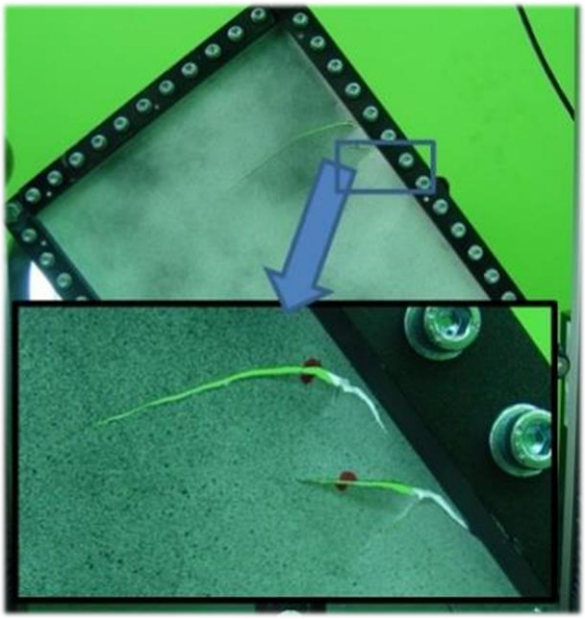


Fig. 12. Fatigue cracks and their location on the plate surface. View from unstiffened side.

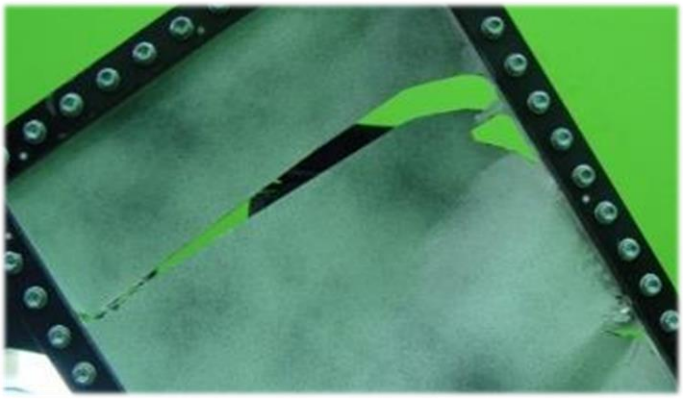


Fig. 13. Structure destruction form after 16,740 load cycles

The deformation caused by the limit load applied to the slab after the end of fatigue tests turned out to be also interesting. In addition to the deepening of the permanent deformation of the slab surface, a method of destroying stiffeners was observed, in which three categories can be distinguished:

- Failure due to local rib buckling and permanent deformation associated with it (Fig. 14a).
- 'Breaking out' of the stiffener from the plate surface due to contact with the loading frame (Fig. 14b).
- A fracture of a rib combined with a brittle fracture caused by the deepening deformation of the transverse surface of the plate (Fig. 14c).

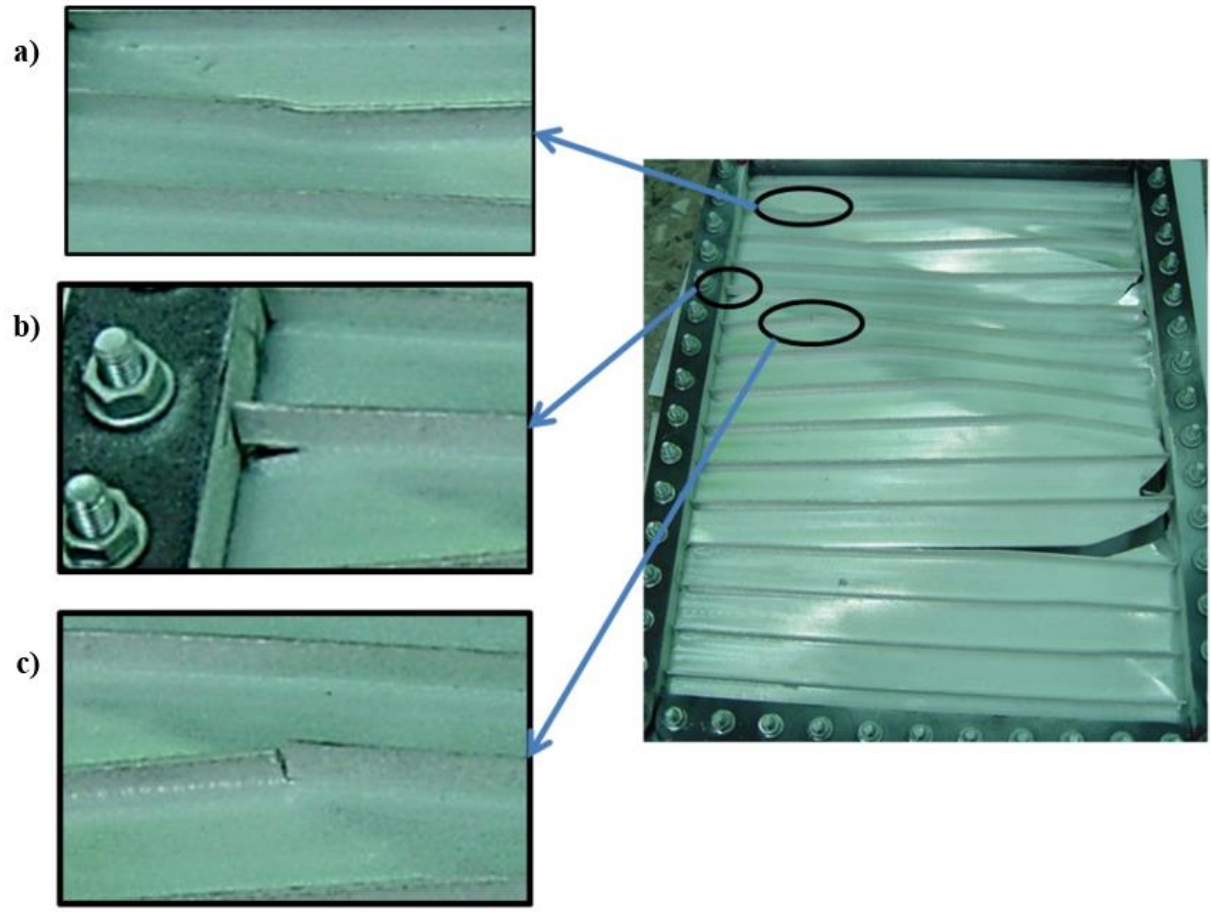


Fig. 14. Observed nature of the failure of the stiffeners

7. CONCLUSIONS

The conducted research shows a significant increase in the operational features of the proposed solution. It was found that without increasing the mass of the structure, it is possible to increase the level of the critical load causing buckling of the structure by 200%. At a given maximum load, a 43% decrease in the value of stress was observed in relation to the base structure in the form of the smooth plate with equivalent mass. The distribution of H-M-H stress and its gradient on the plate surface indicate the advisability of further work on the issue of rational selection of geometric parameters of the integral structure.

Fatigue tests also showed the beneficial effect of stiffeners manifested in the orientation of the fatigue crack. In order to alleviate the stress distribution in the rib-to-skin transition zone, the fillet will be added during the further tests. Such a design correction should show a beneficial effect on the fatigue life of considered structures.

REFERENCES

1. Megson, THG 2014, *Introduction to Aircraft Structural Analysis*, 2nd ed.; Butterworth-Heinemann: Oxford.
2. Niu, MC 2011, *Airframe Structural Design*, 2nd ed.; Conmilit Press Ltd.: Granada Hills, CA.
3. Doyle, JF 2001, *Nonlinear Analysis of Thin-Walled Structures*, Springer-Verlag, Berlin.

4. Quinn, D, Murphy, A, McEwan, W & Lemaitre, F 2009, "Stiffened panel stability behaviour and performance gains with plate prismatic sub-stiffening", *Thin-Walled Structures*, vol. 47, pp. 1457–1468.
5. Quinn, D, Murphy, A & Glazebrook, C 2012, "Aerospace stiffened panel initial sizing with novel skin sub-stiffening features". *International Journal of Structural Stability and Dynamics*, vol. 12, no. 05, 1250060.
6. Shantharaja, M & Srinivas, KR 2014, "Comparison of Riveted Panel and Integral Panel for Damage Tolerance by Using FEA", *International Journal of Science and Research*, vol. 3, no. 9, pp. 426–431.
7. Święch Ł 2019, "Experimental and Numerical Studies of Low-Profile, Triangular Grid-Stiffened Plates Subjected to Shear Load in the Post-Critical States of Deformation", *Materials*, vol. *12*, 3699.
8. Huybrechts, S % Tsai, SW 1996, "Analysis and behaviour of grid structures". *Composite Science and Technol*ogy, vol. *56*, pp. 1101–1015.
9. Bednarz, AS 2020, "Influence of the Amplitude of Resonance Vibrations on Fatigue Life of a Compressor Blade with Simulated FOD Damage", *Advances in Science and Technology Research Journal*, vol. 14, no. 3, pp. 22-29.
10. Sepe, R, Armentani, E, di Lascio, P & Citarella, R 2015, "Crack growth behavior of welded stiffened panel". *Procedia Engineering*, vol. 109, pp. 473–483.
11. GOM GmbH 2019, GOM Software; v.2019; GOM GmbH: Braunschweig.
12. GOM GmbH 2016, *Digital Image Correlation and Strain Computation Basics*; v.2016; GOM GmbH: Braunschweig.
13. Dassault Systemes 2013. *ABAQUS User's & Theory Manuals—Release 6.13-1*; Dassault Systemes: Providence, Rhode Island.
14. Bathe, KJ 1996, *Finite Element Procedures*; Prentice Hall: Upper Saddle River, New York.
15. Doyle, JF 2001, *Nonlinear Analysis of Thin-Walled Structures*; Springer: Luxembourg.
16. Felippa, CA 1987, *Procedures for Computer Analysis of Large Nonlinear Structural System in Large Engineering Systems*; Pergamon Press: London.